LETTER

doi:10.1038/nature10719

Global landscape of HIV–human protein complexes

Stefanie Jäger[1,2], Peter Cimermancic[2,3], Natali Gulbahce[1,2], Jeffrey R. Johnson[1,2,4], Kathryn E. McGovern[1,2], Starlynn C. Clarke[5], Michael Shales[1,2], Gaelle Mercenne[6], Lars Pache[7], Kathy Li[1,2,5], Hilda Hernandez[1,2,5], Gwendolyn M. Jang[1,2,8], Shoshannah L. Roth[9], Eyal Akiva[2,3], John Marlett[10], Melanie Stephens[9], Ivan D'Orso[8]†, Jason Fernandes[8], Marie Fahey[1,2], Cathal Mahon[1,2,5], Anthony J. O'Donoghue[5], Aleksandar Todorovic[11], John H. Morris[5], David A. Maltby[5], Tom Alber[12], Gerard Cagney[13], Frederic D. Bushman[9], John A. Young[10], Sumit K. Chanda[7], Wesley I. Sundquist[6], Tanja Kortemme[2,3,14], Ryan D. Hernandez[2,3,14], Charles S. Craik[2,5], Alma Burlingame[2,5], Andrej Sali[2,3,5,14], Alan D. Frankel[2,8,14] & Nevan J. Krogan[1,2,4,14]

Human immunodeficiency virus (HIV) has a small genome and therefore relies heavily on the host cellular machinery to replicate. Identifying which host proteins and complexes come into physical contact with the viral proteins is crucial for a comprehensive understanding of how HIV rewires the host's cellular machinery during the course of infection. Here we report the use of affinity tagging and purification mass spectrometry[1–3] to determine systematically the physical interactions of all 18 HIV-1 proteins and polyproteins with host proteins in two different human cell lines (HEK293 and Jurkat). Using a quantitative scoring system that we call MiST, we identified with high confidence 497 HIV–human protein–protein interactions involving 435 individual human proteins, with ~40% of the interactions being identified in both cell types. We found that the host proteins hijacked by HIV, especially those found interacting in both cell types, are highly conserved across primates. We uncovered a number of host complexes targeted by viral proteins, including the finding that HIV protease cleaves eIF3d, a subunit of eukaryotic translation initiation factor 3. This host protein is one of eleven identified in this analysis that act to inhibit HIV replication. This data set facilitates a more comprehensive and detailed understanding of how the host machinery is manipulated during the course of HIV infection.

A map of the physical interactions between proteins within a particular system is necessary for studying the molecular mechanisms that underlie the system. The analysis of protein–protein interactions (PPIs) has been successfully accomplished in different organisms using a variety of technologies, including mass spectrometry approaches[1,3,4] and those designed to detect pairwise physical interactions, including the two-hybrid yeast system[5,6] and protein-fragment complementation assays[7]. Although two-hybrid methodologies have been used to systematically study host–pathogen interactions[8,9], so far no systematic affinity tagging/purification mass spectrometry (AP–MS) study has been carried out on any host–pathogen system. Here we have targeted HIV-1 for such an analysis, uncovering a wide variety of host proteins, complexes and pathways that are hijacked by the virus during the course of infection.

We aimed to identify host proteins associated with HIV-1 proteins systematically and quantitatively using an AP–MS approach[2,3]. To this end, we cloned the genes corresponding to all 18 HIV-1 proteins and polyproteins, including the accessory factors (Vif, Vpu, Vpr and Nef), Tat, Rev, the polyproteins (Gag, Pol and Gp160) and the corresponding processed products (MA, CA, NC and p6; PR, RT and IN; and Gp120 and Gp41, respectively) (Supplementary Fig. 1 and Supplementary Table 1). Each clone was fused to a purification tag (consisting of 2×Strep and 3×Flag) and transiently transfected into HEK293 cells; each also was used to generate stably expressed, tetracycline-inducible, affinity-tagged versions of the proteins in Jurkat cells (Fig. 1a and Supplementary Fig. 2). Following multiple purifications of each factor from both cell lines, the material on the anti-FLAG or Strep-Tactin beads, as well as the eluted material, was analysed by mass spectrometry (Fig. 1a and Supplementary Table 2). Finally, an aliquot of each purified factor was subjected to SDS–polyacrylamide gel electrophoresis, stained (Supplementary Fig. 3) and subjected to analysis by mass spectrometry.

For each HIV factor, we identified co-purifying host proteins that were reproducible regardless of the protocol used (Supplementary Figs 4, 5 and 7 and Supplementary Data 1). Several scoring systems can quantify PPIs from AP–MS proteomic data sets, including PE[10], CompPASS[4] and SAINT[11]. For this data set, we devised a scoring system particularly suited for identifying AP–MS-derived host–pathogen PPIs, which we call MiST (mass spectrometry interaction statistics). The MiST score is a weighted sum of three measures: protein abundance measured by peak intensities from the mass spectrum (abundance); invariability of abundance over replicated experiments (reproducibility); and uniqueness of an observed host–pathogen interaction across all viral purifications (specificity) (Fig. 1b and Supplementary Methods). These three metrics are summed by principal component analysis into a composite score (Fig. 1c and Supplementary Data 2). By comparing our dataset with a benchmark of well-characterized HIV–human PPIs (Supplementary Table 3), analysis of the MiST scoring system revealed superior performance on our data set when compared to CompPASS or SAINT (Supplementary Fig. 6) (and comparable performance using other data sets (Supplementary Fig. 8)) and allowed us to define a MiST cut-off of 0.75, corresponding to ~4% of all detected interactions. To estimate how many interactions would exceed this threshold by chance, we randomly shuffled our data set 1,000 times. A random MiST score of 0.75 or greater was assigned to an interaction ten times less frequently than we saw among the MiST scores for the real data, and the probability of an interaction assignment with a random MiST score greater than 0.75 was 2.5×10^{-4} (Fig. 1d).

At the MiST threshold of 0.75, the number of host proteins we found associated with each HIV protein ranged from 0 (CA and p6) to 63 (Gp160) (Fig. 1e). In total, we observed 497 different HIV–human PPIs (347 and 348 identified from HEK293 cells and Jurkat cells, respectively) (Supplementary Data 3). We detected 196 interactions (~40%) in both cell types; 150 and 151 were specific to the HEK293 cells and the Jurkat cells, respectively (Fig. 1e). Only some of these

[1]Department of Cellular and Molecular Pharmacology, University of California, San Francisco, California 94158, USA. [2]California Institute for Quantitative Biosciences, QB3, San Francisco, California 94158, USA. [3]Department of Bioengineering and Therapeutic Sciences, University of California, San Francisco, California 94158, USA. [4]J. David Gladstone Institutes, San Francisco, California 94158, USA. [5]Department of Pharmaceutical Chemistry, University of California, San Francisco, California 94158, USA. [6]Department of Biochemistry, University of Utah, Salt Lake City, Utah 84112, USA. [7]Sanford-Burnham Medical Research Institute, La Jolla, California 92037, USA. [8]Department of Biochemistry and Biophysics, University of California, San Francisco, California 94158, USA. [9]Department of Microbiology, University of Pennsylvania, Philadelphia, Pennsylvania 19104, USA. [10]The Salk Institute for Biological Studies, La Jolla, California 92037, USA. [11]Department of Chemistry, University of California, Berkeley, California 94720, USA. [12]Department of Molecular and Cell Biology, University of California, Berkeley, California 94720, USA. [13]Conway Institute, University College Dublin, Belfield, Dublin 4, Ireland. [14]Host Pathogen Circuitry Group, University of California, San Francisco, California 94158, USA. †Present address: Department of Microbiology, University of Texas Southwestern Medical Center, Dallas, Texas, USA, 75390

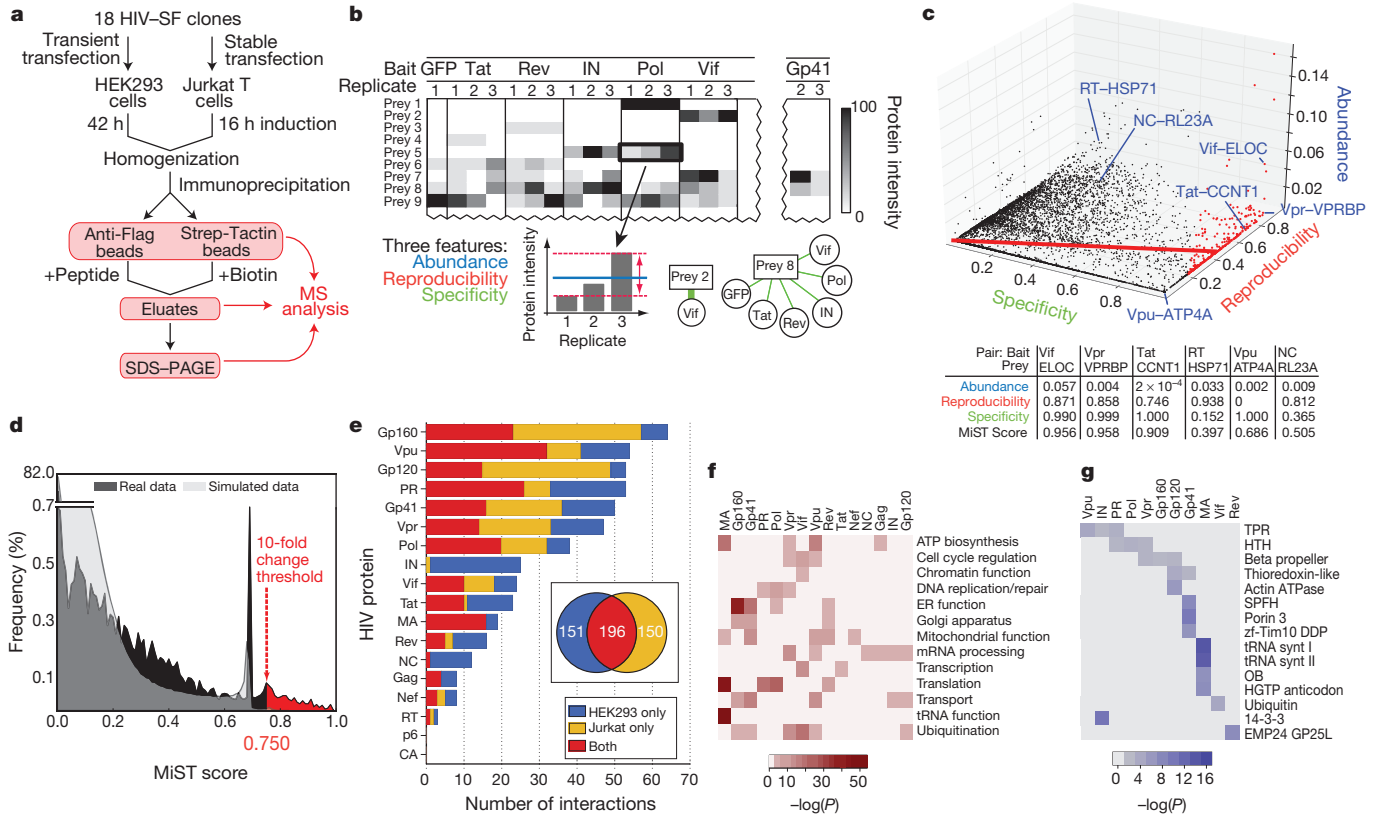

Figure 1 | Affinity purification of HIV-1 proteins, analysis and scoring of mass spectrometry data. **a**, Flowchart of the proteomic AP–MS used to define the HIV–host interactome. PAGE, polyacrylamide gel electrophoresis. SF, 2×Strep–3×Flag affinity tag. **b**, Data from AP–MS experiments are organized in an interaction table with cells representing amount of prey protein purified (for example spectral counts or peptide intensities). Three features are used to describe bait–prey relationships: abundance (blue), reproducibility (the invariability of bait–prey pair quantities; red) and specificity (green). **c**, All bait–prey pairs are mapped into the three-feature space (abundance, reproducibility and specificity). The MiST score is defined as a projection on the first principal component (red line). All interactions, represented as nodes, above the defined threshold (0.75) are shown in red. This procedure separates the interactions more likely to be biologically relevant (for example Vif–ELOC (ELOC also known as TCEB1), Vpr–VPRBP and Tat–CCNT1) from the interactions that are likely to be less relevant owing to low reproducibility (Vpu–ATP4A) or specificity (RT–HSP71 (HSP71 also known as HSPA1A) and NC–RL23A (RL23A also known as RPL23A)). **d**, The histogram of MiST scores (real data) is compared with a randomized set of scores obtained from randomly shuffling the bait–prey table (simulated data). The MiST score threshold (0.75) was defined using a benchmark (Supplementary Table 3) whereby the predictions are enriched for these interactions by a factor of at least ten relative to random predictions (as well as through ROC (receiver operating characteristic) and recall plots (Supplementary Fig. 6)). **e**, Bar graph of the number of host proteins we found interacting with each HIV factor (MiST score, >0.75). The cell type in which the interaction was found is represented in blue (HEK293 only), yellow (Jurkat only) or red (both). **f**, **g**, Heat maps representing enriched biological functions (**f**) and domains (**g**) from the human proteins identified as interacting with HIV proteins (Supplementary Methods). ER, endoplasmic reticulum; mRNA, messenger RNA; tRNA, transfer RNA. TPR, tetratricopeptide repeat; HTH, helix-turn-helix; SPFH, stomatin–prohibitin–flotillin–HflK/C.

specificities could be explained by differential gene expression in the two cell lines (Supplementary Fig. 9). Using antibodies against 26 of the human proteins, and affinity-tagged versions of an additional 101, we could confirm 97 of the 127 AP–MS derived HIV–human PPIs using co-immunoprecipitation/western blot analysis (76% success rate) (Supplementary Figs 10 and 11), suggesting that we derived a high-quality physical interaction data set.

We next analysed the functional categories of host proteins associated with each HIV protein, and in doing so uncovered many expected connections. These included an enrichment of host factors involved in transcription physically linked to the HIV transcription factor Tat and an enrichment of host machinery implicated in the regulation of ubiquitination associating with Vpu, Vpr and Vif, HIV accessory factors that hijack ubiquitin ligases[12] (Fig. 1f and Supplementary Data 4). When we considered domain types instead of whole proteins (Fig. 1g and Supplementary Table 4), we found that host proteins interacting with IN are enriched in 14-3-3 domains, which generally bind phosphorylated regions of proteins[13], and that proteins containing β-propellers have a higher propensity for binding to Vpr (for additional domain enrichment analysis, see Supplementary Fig. 12). These domain analyses could facilitate future structural modelling of HIV–human PPIs.

Next we compared our data to other HIV-related data sets, including previously published HIV–human PPIs and host factors implicated in HIV function from genome-wide RNA interference (RNAi) screens. For example, the VirusMint database[14] contains 587 HIV–human literature-curated PPIs (Supplementary Data 5), which are mostly derived from small-scale, targeted studies. Although the overlap between the 497 interactions identified in this work and those in VirusMint is statistically significant ($P = 8 \times 10^{-8}$), it corresponds to only 19 PPIs (Fig. 2a and Supplementary Table 5). However, a greater overlap exists, one that remains statistically significant, when interactions below the MiST threshold of 0.75 are considered using a sliding cut-off (for example, at a MiST score of 0.2 there exists an overlap of 67 PPIs ($P = 1 \times 10^{-3}$); Fig. 2c, red lines, and Supplementary Data 6). This overlap indicates that we have indeed identified many interactions that have been previously reported. However, it is likely that the higher scoring interactions identified here have a greater chance of being biologically relevant with respect to HIV function than do many of those in VirusMint.

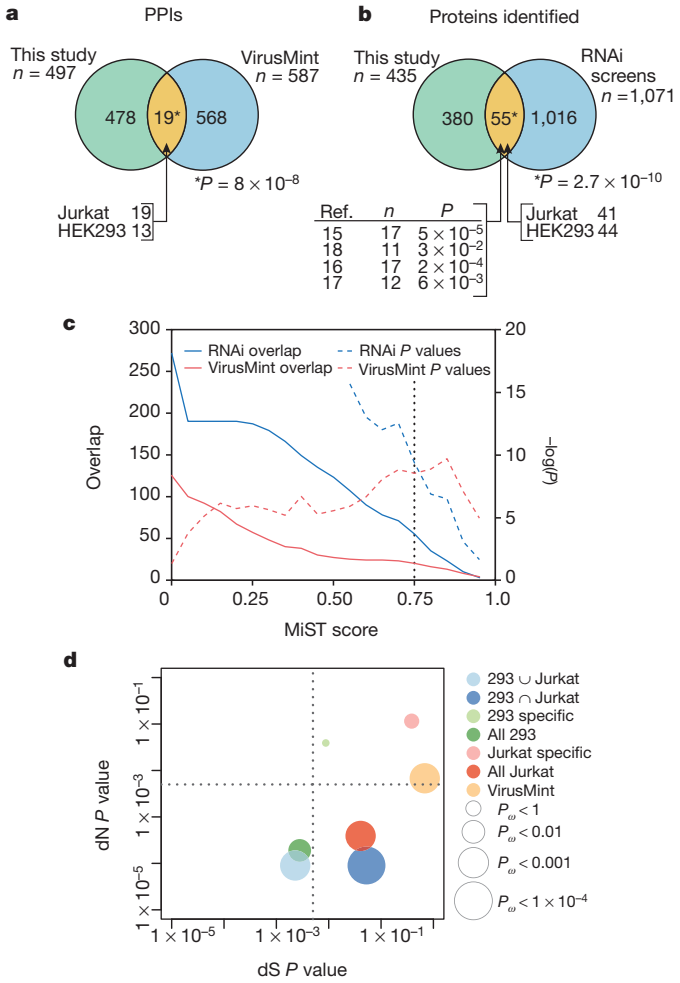

Figure 2 | Comparison of PPI data with other HIV data sets. **a**, Overlap of the 497 HIV–human PPIs with the 587 PPIs reported in VirusMint (Supplementary Table 5). **b**, Overlap of the 435 human proteins with the genes identified in four HIV-dependency RNAi screens[15–18] (Supplementary Table 6). **c**, Number of interactions overlapping with VirusMint (solid red line) and proteins with RNAi screens (solid blue line) as functions of the MiST cut-off. The *P* values of the overlap are represented as dashed lines using the same colours (Supplementary Data 6 and 8). **d**, Comparative genomics analysis of divergence patterns between human and rhesus macaque reveals strong evolutionary constraints on human proteins binding to HIV proteins. The *x* and *y* axes represent *P* values for the synonymous (dS) and non-synonymous (dN) rates of evolution (Supplementary Methods). Horizontal and vertical dotted lines are drawn at 0.5% to indicate the Bonferroni significance threshold for each axis. For the VirusMint data, the significance of ω (dN/dS) is primarily driven by higher rates of synonymous evolution. $\cup$, union; $\cap$, intersection; P_ω, bootstrap-based *P* value for ω.

Recently, four RNAi screens identified host factors that have an adverse effect on HIV-1 replication when knocked down[15–18]. In total, 1,071 human genes were identified in these four studies (Supplementary Data 7), 55 of which overlap with the 435 proteins ($P = 2.7 \times 10^{-10}$; Fig. 2b, Supplementary Fig. 12 and Supplementary Table 6). Again, this overlap increases (as does its statistical significance) if we consider proteins participating in HIV–human PPIs with MiST scores below 0.75 (Fig. 2c, blue lines, and Supplementary Data 8).

To identify the evolutionary forces operating on host proteins interacting with HIV-1, we performed a comparative genomics analysis of divergence patterns between human and rhesus macaque. The proteins identified in both HEK293 and Jurkat cell lines had stronger signatures of evolutionary constraint than those identified exclusively in one cell line or in VirusMint (Fig. 2d). Points in the lower-right quadrant of Fig. 2d show signatures of strong purifying selection, whereas the upper-right quadrant shows signatures more consistent with neutral evolution. This observation suggests that the PPIs identified in our study, especially the ones identified in both cell types, are more physiologically relevant to mammalian evolution than those reported in VirusMint.

We next plotted the 497 HIV–human interactions identified in this study in a network representation (Fig. 3) containing nodes corresponding to 16 HIV (yellow) and 435 human factors that were derived from the HEK293 cells (blue), Jurkat cells (red) or both. We also introduced 289 interactions between human proteins (black edges) derived from several databases[19,20] (Supplementary Data 9). These human–human interactions helped to identify many host complexes, including several that have been previously characterized (see Supplementary Information for a detailed discussion of the HIV–human interaction data sets). Ultimately, all data will be accessible for searching and comparison to other HIV-related data sets using the web-based software GPS-PROT[21] (http://www.gpsprot.org/).

Notably, we found that Pol and PR, which we needed to make catalytically inactive (Supplementary Fig. 1), bound the translational initiation complex eIF3, a 13-subunit complex (eIF3a to eIF3m). We detected 12 of the subunits bound to Pol and/or PR, except eIF3j, which is only loosely associated with the complex[22] (Fig. 4a). Even though PR is the smallest of the *pol*-encoded proteins, we find it associated with the greatest number of host factors (Fig. 4a). To determine whether components of the translation complex are substrates for PR, FLAG-tagged versions of ten eIF3 subunits were individually co-transfected, each with a small amount of active HIV-1 PR, into HEK293 cells. The cell lysates were analysed by western blotting and only eIF3d was found to be cleaved (Fig. 4b). Purification of tagged versions of the amino and carboxy termini of cleaved eIF3d revealed that only the N terminus of 114 amino-acid residues associates with the eIF3 complex (Supplementary Table 7). The cleavage occurred with an efficiency similar to that of the processing of the natural PR substrate Gag (Fig. 4c), whereas two cellular proteins previously described to be cleaved by HIV PR, PAPBC1[23] and BCL2[24], were cleaved only at higher PR concentrations or not at all, respectively. To confirm this result *in vitro*, we incubated purified human eIF3 with active PR, resulting in the removal of a 70-kDa band and the appearance of a ~60-kDa protein product (Fig. 4d). Analysis of the cleaved product by N-terminal sequencing revealed a cleavage of eIF3d between Met 114 and Leu 115, which corresponds to the consensus sequence for HIV-1 protease[25] and falls within the RNA-binding domain (RRM) of eIF3d (ref. 26; Fig. 4d).

Next we used four to six short interfering RNAs against different eIF3 subunits in HIV infectivity assays (Fig. 4e, f, Supplementary Fig. 14 and Supplementary Table 8). Using a fusion of HIV with vesicular stomatitis virus glycoprotein (VSV-G), which only allows for a single round of replication, knockdown of eIF3d, but not other eIF3 subunits, resulted in an increase in infectivity (Fig. 4e), suggesting that this factor acts in early stages of infection. In assays requiring multiple rounds of HIV infection, knockdown of eIF3d, eIF3e and eIF3f enhanced HIV NL4.3 infectivity by a factor of three to five, whereas inhibition of eIF3c, eIF3g and eIF3i had no promoting effect (Fig. 4f). Consistent with these results, a previous overexpression screen for factors that restrict HIV-1 replication identified eIF3f as the most potent inhibitory clone[27]. Furthermore, using assays monitoring both early and late products we found that knockdown of eIF3d results in an increase in accumulation of reverse transcription product (Fig. 4g and Supplementary Fig. 15). This suggests that eIF3 does in fact have a role in the early stages of infection, perhaps by binding to the viral RNA through the RNA-binding domain in eIF3d, and thus inhibiting RT, an effect that is overcome by PR cleavage of eIF3d (Supplementary Fig. 16). These results suggest that our data set will be enriched not only for host proteins the virus requires for efficient replication (Fig. 2b, c), but also those that have an inhibitory role during infection. Indeed, we have found that an additional ten factors from our list of interactors, when knocked down by RNAi, produce an increase in HIV infection (Supplementary Figs 17–19, Supplementary Tables 12

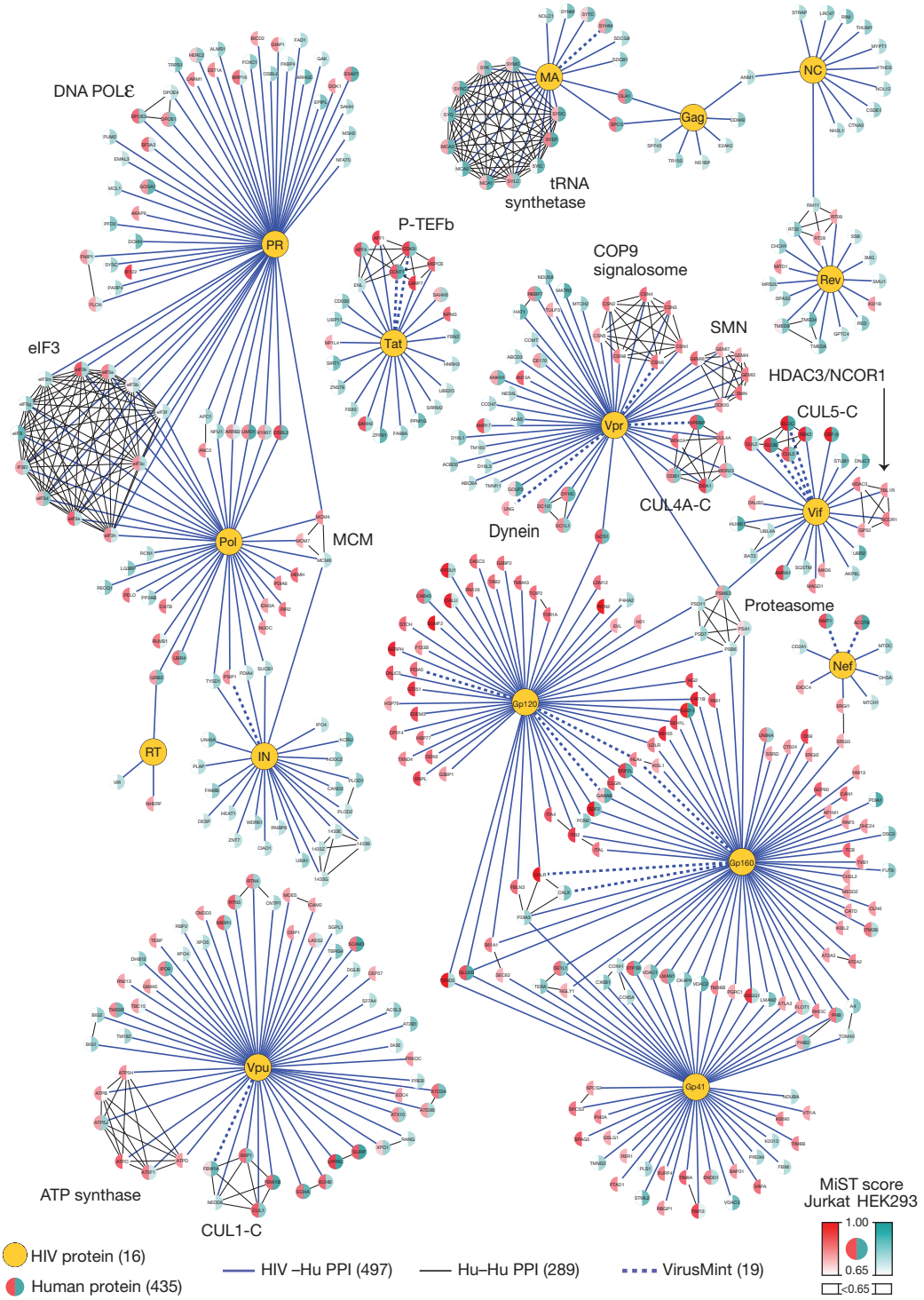

Figure 3 | Network representation of the HIV–human PPIs. In total, 497 HIV–human interactions (blue) are represented between 16 HIV proteins and 435 human factors. Each node representing a human protein is split into two colours and the intensity of each colour corresponds to the MiST score from interactions derived from HEK293 (blue) or Jurkat (red) cells. Black edges correspond to interactions between host factors (289) that were obtained from publicly available databases; dashed edges correspond to interactions also found in VirusMint[14].

and 13 and Supplementary Methods). Knockdown of two of these, DESP and HEAT1, also resulted in an increase in HIV integration (Supplementary Fig. 20 and Supplementary Table 14), consistent with their physical association with IN.

As well as performing the systematic AP–MS study reported here, we explored in further detail the biological significance of two newly identified HIV–human interactions: HIV protease targeting a component of eIF3 that is inhibitory to HIV replication; and CBF-β, a new component of the Vif–CUL5 ubiquitin ligase complex required for APOBEC3G stability and HIV infectivity[28]. Further work will be required to determine whether, how and at what stage of infection the remaining host factors impinge on HIV function. Ultimately, our analysis of the host factors co-opted by different viruses using the same proteomic pipeline will allow for the identification of protein complexes routinely targeted by different pathogens, which may represent better therapeutic targets for future studies.

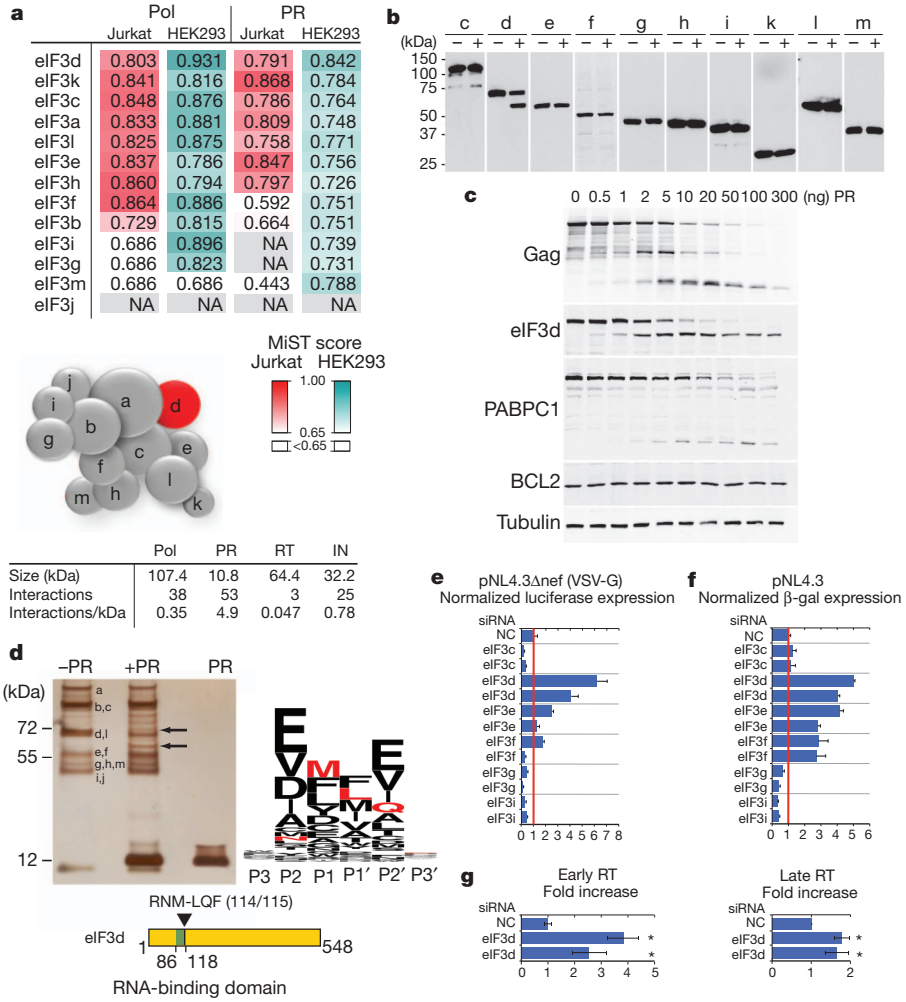

Figure 4 | eIF3d is cleaved by HIV-1 PR and inhibits infection. **a**, MiST scores for eIF3 subunits associated with PR (right) and Pol (left) in HEK293 and Jurkat cells. Sizes of the proteins and numbers of significant interactions (MiST score, >0.75) detected for Pol and its subunits are shown below, as is a modular representation of the eIF3 complex[29]. The cleaved subunit, eIF3d, is in red. **b**, Western blot of HEK293 cell lysate expressing FLAG-tagged eIF3 subunits in the absence (−) or presence (+) of active PR probed with an anti-FLAG antibody. **c**, HEK293 cells were co-transfected with Gag, or FLAG-tagged eIF3d, PABPC1, BCL2 and increasing amounts of PR. Cell lysates were probed against Gag (upper panel), FLAG-tagged eIF3d (middle panel) or tubulin as control (lower panel). **d**, Silver stain of purified eIF3 complex incubated with recombinant HIV-1 PR. The residues corresponding to the eIF3d cleavage site (red) is located within the RNA-binding domain[26]. **e**, **f**, HeLa-derived P4/R5 MAGI cells were transfected with two different short interfering RNAs (siRNAs) targeting individual subunits of the eIF3 complex (Supplementary Tables 7 and 9) and subsequently infected with either a pNL4-3-derived, VSV-G-pseudotyped, single-cycle virus (HIV–VSV-G) (**e**) or wild-type pNL4-3 (**f**). NC, negative control. **g**, Early (left) and late (right) HIV-1 DNA levels measured by quantitative PCR amplification in cells transfected with two independent eIF3d siRNAs or with control siRNAs. Samples were normalized by input DNA amount or by cellular gene (*HMBS*) copy number. The RT and replication assays were done three to five times and the standard deviations are shown (Supplementary Tables 7, 10 and 11). *$P < 0.05$ (Kruskal–Wallis test with Dunn's correction for multiple comparisons).

METHODS SUMMARY

More details on experimental assays, plasmid constructs, sequences, cell lines, antibodies and computational analysis are provided in Supplementary Methods. Briefly, affinity tagging and purification was carried out as previously described[2] and the protein samples were analysed on a Thermo Scientific LTQ Orbitrap XL mass spectrometer. For the evolutionary analysis, genome-wide alignments to rhesus macaque were downloaded from the University of California, Santa Cruz genome browser (http://genome.ucsc.edu/) and evolutionary rates for each group of genes considered were measured using the synonymous and non-synonymous rates of evolution. For the *in vitro* protease assay, maltose binding protein (MBP)-tagged PR was expressed in BL21 (Gold) DE3 cells in the presence of 100 μM Saquinavir and purified on an MBP trap column. Purified eIF3 was obtained from J. Cate (University of California, Berkeley). For the infection assays, HeLa P4.R5 cells were transfected with short interfering RNAs and after 48 h infected with pNL4-3 or a pNL4-3-derived VSV-G-pseudotyped reporter virus. Infection levels were determined by luminescence read-out.

Received 26 March; accepted 18 November 2011.
Published online 21 December 2011.

1. Gavin, A. C. *et al.* Proteome survey reveals modularity of the yeast cell machinery. *Nature* **440,** 631–636 (2006).
2. Jäger, S. *et al.* Purification and characterization of HIV-human protein complexes. *Methods* **53,** 13–19 (2011).
3. Krogan, N. J. *et al.* Global landscape of protein complexes in the yeast *Saccharomyces cerevisiae*. *Nature* **440,** 637–643 (2006).
4. Sowa, M. E., Bennett, E. J., Gygi, S. P. & Harper, J. W. Defining the human deubiquitinating enzyme interaction landscape. *Cell* **138,** 389–403 (2009).
5. Yu, H. *et al.* High-quality binary protein interaction map of the yeast interactome network. *Science* **322,** 104–110 (2008).
6. Stelzl, U. *et al.* A human protein-protein interaction network: a resource for annotating the proteome. *Cell* **122,** 957–968 (2005).
7. Tarassov, K. *et al.* An *in vivo* map of the yeast protein interactome. *Science* **320,** 1465–1470 (2008).
8. Calderwood, M. A. *et al.* Epstein-Barr virus and virus human protein interaction maps. *Proc. Natl Acad. Sci. USA* **104,** 7606–7611 (2007).

9. Shapira, S. D. *et al.* A physical and regulatory map of host-influenza interactions reveals pathways in H1N1 infection. *Cell* **139,** 1255–1267 (2009).
10. Collins, S. R. *et al.* Toward a comprehensive atlas of the physical interactome of *Saccharomyces cerevisiae. Mol. Cell. Proteomics* **6,** 439–450 (2007).
11. Choi, H. *et al.* SAINT: probabilistic scoring of affinity purification-mass spectrometry data. *Nature Methods* **8,** 70–73 (2011).
12. Malim, M. H. & Emerman, M. HIV-1 accessory proteins–ensuring viral survival in a hostile environment. *Cell Host Microbe* **3,** 388–398 (2008).
13. Yaffe, M. B. *et al.* The structural basis for 14-3-3:phosphopeptide binding specificity. *Cell* **91,** 961–971 (1997).
14. Chatr-aryamontri, A. *et al.* VirusMINT: a viral protein interaction database. *Nucleic Acids Res.* **37,** D669–D673 (2009).
15. Brass, A. L. *et al.* Identification of host proteins required for HIV infection through a functional genomic screen. *Science* **319,** 921–926 (2008).
16. König, R. *et al.* Global analysis of host-pathogen interactions that regulate early-stage HIV-1 replication. *Cell* **135,** 49–60 (2008).
17. Yeung, M. L., Houzet, L., Yedavalli, V. S. & Jeang, K. T. A genome-wide short hairpin RNA screening of Jurkat T-cells for human proteins contributing to productive HIV-1 replication. *J. Biol. Chem.* **284,** 19463–19473 (2009).
18. Zhou, H. *et al.* Genome-scale RNAi screen for host factors required for HIV replication. *Cell Host Microbe* **4,** 495–504 (2008).
19. Ruepp, A. *et al.* CORUM: the comprehensive resource of mammalian protein complexes–2009. *Nucleic Acids Res.* **38,** D497–D501 (2010).
20. Stark, C. *et al.* BioGRID: a general repository for interaction datasets. *Nucleic Acids Res.* **34,** D535–D539 (2006).
21. Fahey, M. E. *et al.* GPS-Prot: a web-based visualization platform for integrating host-pathogen interaction data. *BMC Bioinformatics* **12,** 298 (2011).
22. Hinnebusch, A. G. eIF3: a versatile scaffold for translation initiation complexes. *Trends Biochem. Sci.* **31,** 553–562 (2006).
23. Alvarez, E., Castello, A., Menendez-Arias, L. & Carrasco, L. HIV protease cleaves poly(A)-binding protein. *Biochem. J.* **396,** 219–226 (2006).
24. Strack, P. R. *et al.* Apoptosis mediated by HIV protease is preceded by cleavage of Bcl-2. *Proc. Natl Acad. Sci. USA* **93,** 9571–9576 (1996).
25. Schilling, O. & Overall, C. M. Proteome-derived, database-searchable peptide libraries for identifying protease cleavage sites. *Nature Biotechnol.* **26,** 685–694 (2008).
26. Asano, K. *et al.* Structure of cDNAs encoding human eukaryotic initiation factor 3 subunits. Possible roles in RNA binding and macromolecular assembly. *J. Biol. Chem.* **272,** 27042–27052 (1997).
27. Valente, S. T., Gilmartin, G. M., Mott, C., Falkard, B. & Goff, S. P. Inhibition of HIV-1 replication by eIF3f. *Proc. Natl Acad. Sci. USA* **106,** 4071–4078 (2009).
28. Jäger, S. *et al.* Vif hijacks CBF-β to degrade APOBEC3G and promote HIV-1 infection. *Nature* http://dx.doi.org/10.1038/nature10693 (this issue).
29. Zhou, M. *et al.* Mass spectrometry reveals modularity and a complete subunit interaction map of the eukaryotic translation factor eIF3. *Proc. Natl Acad. Sci. USA* **105,** 18139–18144 (2008).

Supplementary Information is linked to the online version of the paper at www.nature.com/nature.

Acknowledgements We thank A. Choi, Z. Rizvi and E. Kwon for cloning of human genes and J. Cate for purified eIF3. We also thank J. Gross, R. Andino, R. Harris, M. Daugherty and members of the Krogan lab for discussion. This research was funded by grants from QB3@UCSF and the National Institutes of Health (P50 GM082250 to N.J.K., A.D.F., C.S.C. and T.A.; P01 AI090935 to N.J.K., S.K.C., J.A.Y. and F.D.B.; P50 GM081879 to N.J.K. and A.B.; P50 GM082545 to W.I.S.; P41RR001614 to A.B.; U54 RR022220 to A.S.; P01 GM073732-05 to A.T.; CHRP-ID08-TBI-063 to S.K.C.; P41 RR001081 to J.H.M.) and from the Nomis Foundation (to J.A.Y.). N.J.K. is a Searle Scholar and a Keck Young Investigator.

Author Contributions S.J. generated the protein–protein interaction map; P.C. developed the MiST scoring system; N.G., M. Shales, E.A., M.F., J.H.M., J.R.J. and R.D.H. provided computational support; K.E.M., K.L., J.R.J., H.H., G.M.J., I.D., J.F. and D.A.M. provided experimental support; S.J., S.C.C., A.J.O. and A.T. characterized the PR–eIF3d interaction; S.J., G.M.J., C.M. and G.M. confirmed the interactions by immunoprecipitation/western blot; L.P., S.L.R., J.M. and M. Stephens used RNAi for functional verification; T.A., G.C., F.D.B., J.A.Y., S.K.C., W.I.S., T.K., R.D.H., C.S.C., A.B., A.S., A.D.F. and N.J.K. supervised the research; and S.J., P.C., A.S. and N.J.K. wrote the manuscript.

Author Information Reprints and permissions information is available at www.nature.com/reprints. The authors declare no competing financial interests. Readers are welcome to comment on the online version of this article at www.nature.com/nature. Correspondence and requests for materials should be addressed to N.J.K. (krogan@cmp.ucsf.edu).